

Differential Thermal Inertia of Geological Surfaces

Sabol, Donald E.¹, Gillespie, Alan R.¹, McDonald, Eric², and Danilina, Iryna¹

¹ Dept of Earth & Space Sciences, University of Washington, Seattle, Washington, USA, 98195

² Earth & Ecosystems Science, Desert Research Institute, Reno, Nevada, USA, 89512

Don Sabol (don@rad.ess.washington.edu), Alan Gillespie (arg3@u.washington.edu), Eric McDonald (Eric.McDonald@dri.edu), Iryna Danilina (danilina@u.washington.edu)

ABSTRACT

In terrestrial remote sensing, thermal inertia has been little used because its calculation involves registered albedo, day-night TIR, and DEM images, and its value is sensitive to vegetation, transient cloudiness and wind. We explore a technique in which $\Delta T/\Delta t \approx dT/dt$ (the rate of temperature change) is measured for short time intervals and used to estimate thermal inertia, reducing the opportunity for cloudiness, wind or rainfall to disrupt the experiment. It has its maximum/minimum values in the morning/afternoon, instead of noon/midnight for the conventional approach. These characteristics make for a better experimental design. In this study we use a FLIR TIR camera to evaluate "differential" thermal inertia relative to values from day/night algorithms for a playa (Soda Lake) and environs in the Mojave Desert of California. For the FLIR, $NE\Delta T \approx 0.2$ K, and we use 10-s time bursts of video-rate measurements to reduce this value an order of magnitude and continued the sampling over a diurnal period. Images were made of wet and dry patches of the playa (monitored by lysimeter and thermocouple profiles) and dry sand and bedrock. We compared theoretical results calculated from heat-diffusion equations to the FLIR measurements. The results suggest that the differential approach can be used to estimate thermal inertia provided that images are acquired 10 min or more apart if $NE\Delta T < 0.02$ K, or an hour apart for current airborne or satellite sensors.

1 INTRODUCTION

Thermal inertia (P) is an important property of geologic surfaces that essentially describes the resistance to temperature change as heat is added, for example from the sun during the day. Most remote-sensing images describe only the surface. However, P is a volume property that is sensitive to the composition of the near surface, down to a depth reached by (for example) the diurnal heating wave (~20 cm). Thermal-inertia mapping (e.g., Gillespie and Kahle, 1977) is sensitive to differences in near-surface density, composition, and porosity.

In terrestrial remote sensing, P has been little used because its calculation involves registered albedo, day-night TIR, and DEM images, and its value is sensitive to vegetation, transient cloudiness and wind. We explore a technique in which $\Delta T/\Delta t \approx dT/dt$ (the rate of temperature change) is measured and used to estimate thermal inertia. dT/dt is proportional to the day/night temperature difference, and hence P . $\Delta T/\Delta t$ can be measured for short time intervals, reducing the opportunity for cloudiness, wind or rainfall to disrupt the experiment. It has its maximum/minimum values in the morning or afternoon, instead of noon/midnight for the conventional approach. The short time scale of

measurement makes for a better experimental design. In this study, we use a FLIR TIR camera to evaluate differential thermal inertia relative to day/night algorithms for a playa (Soda Lake) and environs in the Mojave Desert of California.

2 BACKGROUND

2.1 Thermal Inertia

Thermal inertia (P) is defined as:

$$P = (k \rho C)^{1/2} \quad (1)$$

where k = bulk thermal conductivity [$\text{cal s}^{-1} \text{cm}^{-1} \text{K}^{-1}$]; ρ = bulk density [g cm^{-3}]; C = specific heat capacity [$\text{cal g}^{-1} \text{K}^{-1}$]. It is estimated by comparing temperature differences at different times of day to values predicted by temperature diffusion models (Kahle, 1977). Typically, measurements are made near noon (T_{day}) and midnight (T_{night}) to maximize the contrast. In a simpler approach, Price (1977) defined an approximation of P , the apparent thermal inertia (ATI), calculated as:

$$ATI = (1 - A)/(T_{\text{day}} - T_{\text{night}}) \quad (2)$$

where A = albedo. Figure 1 shows the influence of A on the daily heating curve: as A is decreased from

0.5 to 0.1, more heat is absorbed by the surface, which becomes hotter. The ATI equation (2) suggests that dividing the absorbed energy $(1-A)$ by $(T_{day}-T_{night})$ should be constant ($\sim 0.02 \text{ cal cm}^{-2} \text{ K}^{-1} \text{ s}^{-1/2}$), which can be verified from the data plotted in the figure.

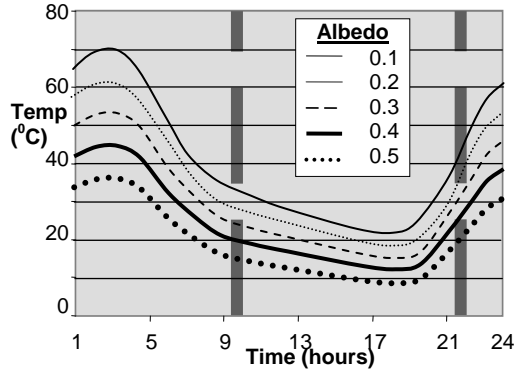


Figure 1: The effect of albedo A on the daily temperature curve when ρ , k , and C (and P) are held constant. Although A has the primary effect of offsetting the day/night temperature curve, $T_{day}-T_{night}$ ranges from 47 to 31 °C as A ranges from 0.1 to 0.5.

For common desert soils, $P \approx 0.024 \text{ cal cm}^{-2} \text{ K}^{-1} \text{ s}^{-1/2}$ (Kahle, 1980), while for basalt and water $P \approx 0.053 \text{ cal cm}^{-2} \text{ K}^{-1} \text{ s}^{-1/2}$ and $\sim 0.038 \text{ cal cm}^{-2} \text{ K}^{-1} \text{ s}^{-1/2}$ respectively. Thermal-inertia contrast depends on the composition of the surface, but also on the proportion of the components in the scene. The contrast is typically sufficient to permit detection of the differential thermal inertia of some geologic materials in images. Even replacing air in soil with water increases P sufficiently that dry and moist soils can be distinguished.

Direct measurement of P is difficult because the values of k , ρ , and C for scene components are usually unknown and cannot be measured remotely. Remote determination of even relative P is complicated by: 1) heterogeneity of materials in the instantaneous field of view; 2) topographic roughness; 3) moisture content; 4) vegetation; and 5) variable local weather conditions (temperature, cloud cover, rainfall, wind) (Van Dam *et al.* 2005). In principle, P can be estimated for image pairs made at a range of time differences: for example, Nash (1988) used seasonal differences instead of diurnal differences to “see” bedrock surfaces buried more deeply ($\sim 50 \text{ cm}$) than detectable ordinarily ($\sim 20 \text{ cm}$). However, in all cases it is necessary to make the images near the peak and trough of the daily or seasonal heating cycle – for example, noon and midnight, or summer and winter, but not dusk and dawn or spring and fall.

2.2 Differential Thermal Inertia

It can be shown using the heat equation:

$$\frac{\partial T}{\partial t} = \frac{K}{\rho \cdot c} \cdot \frac{\partial^2 T}{\partial x^2} \quad (1)$$

that P can be derived from $\partial T/\partial t$. For a periodic external flux (in the simplest case $j = j_0 \sin \omega t$, where j_0 is the amplitude of incoming flux and $\omega = 2\pi/\text{day}$ is the frequency of incoming flux), the amplitude of temperature oscillation is inversely proportional to P :

$$T(0,t) = -\frac{j_0}{\sqrt{\omega/2} \cdot P} \cdot \cos \omega t \quad (2)$$

Accordingly, the amplitude of the derivative is defined by thermal inertia as well, other things being equal:

$$\frac{\partial T}{\partial t} = \frac{j_0 \cdot \omega}{\sqrt{\omega/2} \cdot P} \cdot \sin \omega t \quad (3)$$

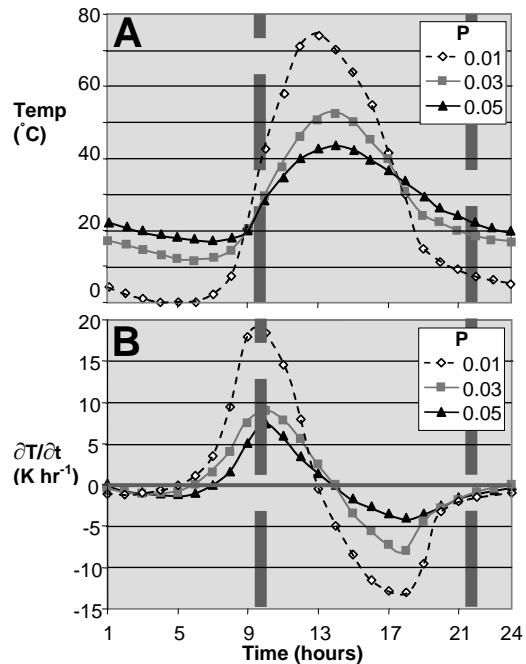


Figure 2: Changes in temperature (A) and the rate of temperature change over time (B) for different thermal inertia values (P). After Kahle (1977). Thick dashed lines show typical satellite overpass times.

Thus, materials with different thermal inertias have different diurnal temperature fluctuations, requiring that $\partial T/\partial t$ also is different, at least at some times of day (Fig. 2). P can be inferred from $\Delta T/\Delta t$ as well as from $T_{day}-T_{night}$, with the notable difference that the optimum times of measurement are morning or

afternoon, when the maximum $|\partial T/\partial t|$ values occur (Fig. 1). Around noon and midnight $\partial T/\partial t \approx 0$, regardless of P .

In the differential approach ΔT is much smaller than for the day/night approach (~ 20 K), and therefore $\Delta T/\Delta t$ is more sensitive to measurement precision ($NE\Delta T$). $NE\Delta T$ is accordingly an important limit recovering P . Essentially, Δt must be long enough that $\Delta T \gg NE\Delta T$. For sensors such as MASTER, with $NE\Delta T \approx 0.3$ K, $\Delta t > 60$ min is commonly required for a signal/noise ratio of >10 in ΔT and in the P image. Although such a low SNR may be acceptable in photointerpretation, it reduces the reliability of quantitative analysis of P ; yet, increasing Δt further reduces both the pragmatic advantages of the differential approach and the ability to estimate $\partial T/\partial t$ meaningfully.

Thermal radiance images can now be measured with precisions better than when the classic terrestrial thermal-inertia studies were made in the 1970s, and this improvement can be used to shorten Δt used while maintaining the same number of meaningful gray levels in the output ATI image. We call the ATI calculated with short Δt values “differential ATI,” or DATI.

3 METHODS

3.1 Study Area

DATI was evaluated on a series of thermal images taken during July 2005 and 2006 of Soda Lake Playa in the Mojave Desert of California, USA. Soda Playa is at the terminus of the Mojave River and is seasonally wet during the year. The river itself is dry at the surface and provides subsurface moisture to parts of the western side of the playa. The surface of the playa is dominated by wind-blown silt that forms a surface crust. Evaporates, primarily sodium carbonate and sodium bicarbonate, form in these crusts and can locally dominate surface composition. In July, the crust of the playa surface is primarily dry, while the subsurface typically has moisture content up to 22% by weight. It is the effect of the subsurface moisture on the thermal inertia of the dry crust surface that was investigated in this study.

3.2 TIR data acquisition

Thermal images were taken every 5 minutes in 10 second time bursts (ten images) with a FLIR Systems ThermaCAM S45 thermal camera from the Desert Studies Center at Zzyzx located on the western edge of the playa. By averaging the radiant measurements over the 10 seconds, we were able to reduce the effective $NE\Delta T$ from 0.2 K to ~ 0.06 K. By averaging consecutive bursts, we were able to calculate values of

dT/dt that were relatively insensitive to fluctuating sensible-heat loss due to wind. This cascaded sampling strategy was continued for a day.

Four patches in the playa were instrumented with data loggers that recorded the subsurface temperature via thermocouples imbedded at depths of 2, 5, 10, and 40 cm. Also, moisture content of the subsurface at these depths was determined by weighing and drying samples collected at each “patch.” The moisture content and subsurface temperatures were used to interpret the FLIR data and derived DATI values.

4 RESULTS / DISCUSSION

4.1 Subsurface Soil Moisture and Temperature

The surface (<0.5 cm depth) of the playa in the analysis is dry ($< 4\%$ moisture by weight). Soil moisture under this “dry skin” was as high as 14%,

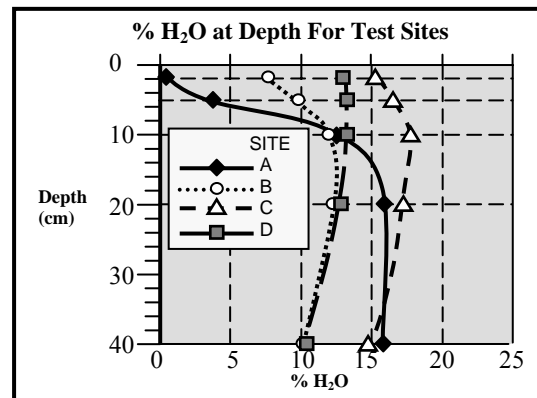


Figure 3: Sub-surface moisture content for four sites at Soda Playa.

depending on the site and depth (Fig. 3). For the purposes of this paper, “wet” and “dry” refer to the moisture content immediately under the surface (1 to 5 cm). Therefore, C and D are “wet” while A is “dry”. Radiant, air, and subsurface soil temperatures at these sites varied during the heating cycle with depth and composition (primarily moisture content). This can be seen in Figure 4, which contrasts the effect of wet and dry soils on the morning heating. The intensity of the heat wave diminished with depth, such that the response is only a few degrees at 40 cm, and occurs hours after initial surface heating. The heating at the surface is more immediate and intense. The increased moisture near the surface diminishes the rate and intensity of heating. It is the rate of heating at the surface/near-surface that is useful for DATI.

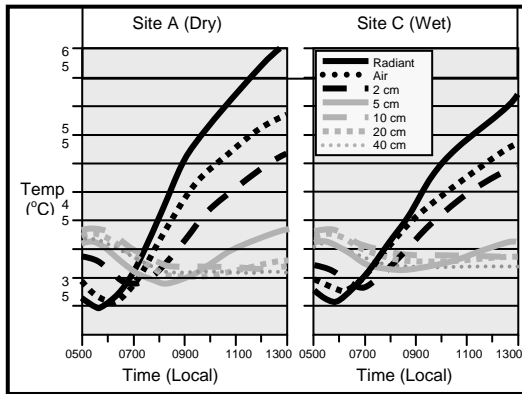


Figure 4: The effect of morning heating of soil at depth for Sites A and C. The radiant temperatures were extracted from a series of FLIR images while sub-surface temperatures were measured with thermocouples.

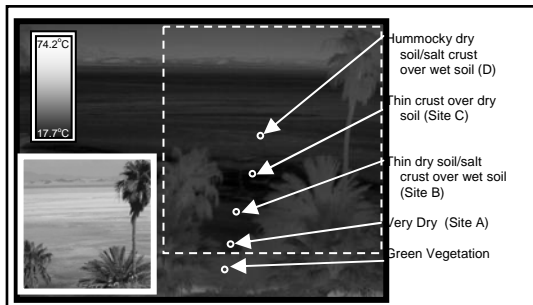


Figure 5: FLIR image of the view towards the east from Zzyzx Desert Studies Center overlooking Soda Lake Playa taken at 0540, 14 July 2006. A B&W photo of the area is inset and depicts the area shown by a dashed box in the FLIR image. This figure is presented as a reference for time series of FLIR images shown in Figure 6.

As soil moisture varies with depth, so does P . Therefore, an effective value of P (more heavily weighted at the surface and diminishing with depth) is all that can be recovered by DATI or ATI.

4.2 Surface Radiant Temperature

The short-term change in surface temperatures of dry and moist subsurface playa soils can be seen in thermal images. Figure 5 is a reference image for the time series shown in Figure 6. The left column of Figure 6 is a time series of FLIR images taken every 20 minutes between 0600 and 0820 during sunrise taken (the same day as Fig. 5). The band of cooler soil in the lower center of the image (marked by an X) is relatively dry, powdery, and hummocky (relative to the surrounding playa surfaces). With its pore spaces filled with more air (as opposed to water), its thermal inertia is lower and, therefore, gets cooler at night.

The difference between the FLIR image in Figure 5 (taken at 0540) and each subsequent time step is shown in the center column of Figure 6. This column essentially shows the incremental effect of thermal inertia over the different surfaces over the period of rapid heating.

Progressive 20-minute temperature differences are shown in the right column of Figure 6. The top image is the difference between the 0540 and 0800 FLIR images and shows little change as the sun has not yet risen over the mountains to the east. Subtle differences in the surface temperatures can be seen in the subsequent 20-minute time steps. A rapid rate of surface heating occurred between 0640 and 0700 (when full sunlight has finally reached the whole scene). Note that the cooler, hummocky area (X) is still warming at a lower rate (darker in Fig. 6) than the surrounding wetter soil up until ~0740. This is counter to what might be expected. This dryer zone should be warming faster than the wetter playa as it has a lower P and, therefore, should respond faster to heating/cooling cycles. This apparent cooling is due to the fact that the image is taken looking east, towards the rising sun. The low sun angle in early morning causes shadows on the rough surface of this zone and the image is looking into those shadows. Hence, not all the surfaces of this dry zone are yet exposed to full sunlight / heating. As the sun continues to rise, this changes and, by 0820, the differential heating shows a relatively rapid temperature rise in this zone. It is, therefore, important to keep other factors, such as surface roughness and direction of solar heating in mind with interpreting DATI images.



Figure 6: Series of FLIR images towards the east of Soda Playa, CA (USA). Gray scale shows temperatures; numbers in upper left are local acquisition times. Left column shows radiance images; center shows different from 0540; and right is the sequential difference.

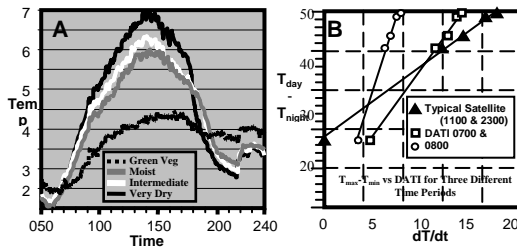


Figure 7: A) Non-smoothed temperature changes for different units from 0500 to midnight, 14 July 2006. B) $T_{day(max)} - T_{night(min)}$ vs DATI for surfaces with different P in the FLIR images of Figure 6.

5 CONCLUSIONS

DATI has the potential to be used to map, and ultimately estimate thermal inertia. Our results indicate that near-surface composition affects the response of the surface to diurnal heating and cooling. Ideal times for measuring DATI are in the morning (from sunrise until ~ 0900) or in the evening (from just before sunset until ~ 2100). If the surfaces are rough, shadows cast at low sun angles can cause some surfaces to appear cooler than equivalent smooth ones, especially when viewed obliquely into the rising/setting sun. Wind and clouds can cause fluctuations in the surface temperature, as seen in Figure 7A (~ 1500 and $2200-2400$). To minimize the variability caused by these short-term temporal fluctuations, image sampling should include several images (5-20) averaged over a 1-2 minute period. Clearly, the longer the time gap between the image pairs for determining DATI, the better (provided the second image is taken during the same heating/cooling episode). It appears that a minimum of 20 minutes in desert environments is necessary, although closer to 2 hours would yield more precise estimates of P .

There is a linear relationship between ATI and DATI, as shown in Figure 7B. Here ATI is plotted against DATI for different times of the morning and different Δt . For each DATI, five areas in the image with different P are plotted. This linear relationship suggests that an effective P may be recovered using DATI.

The slope of the warming curve (smoothed) is shown in Figure 8 for wet and dry playa surfaces. For each of these surfaces, the greatest rate in heating with separation between the heating curves for the different materials is between 0600 and 0700. After 0800, temperature continues to rise, but at a lower rate.

The DATI approach shows promise in that it allows for relatively quick assessment of apparent thermal inertia and reduces affects of changes in climate, clouds, winds, etc., over traditional day/night methods. This makes it more adaptable for field

analysis as well as use with unmanned airborne vehicles. The next step in this study is to convert this rate into predicted day/night apparent thermal inertia and then to estimate thermal inertia.

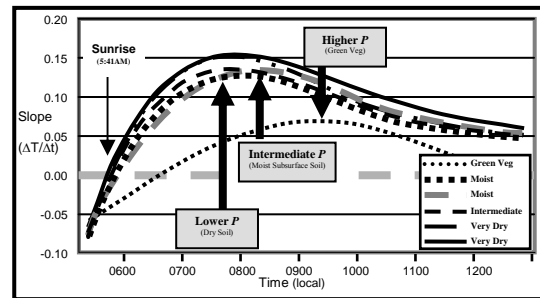


Figure 8: The slope ($\Delta T/\Delta t$) of the temperature change for wet/dry subsurface soils and green vegetation on Soda Playa, CA, 14 July 2006.

6 REFERENCES

- Gillespie, A.R., and Kahle, A., 1977. The construction and interpretation of a digital thermal inertia image. *Photogrammetric Engineering and Remote Sensing* 43(8), 983-1000.
- Kahle, A., 1977. A simple thermal model of the Earth's surface for geologic mapping by remote sensing. *Journal of Geophysical Research* 82, 1673-1680.
- Kahle, A., 1980. Surface Thermal Properties. In *Remote Sensing in Geology*, Siegal, B.S., and Gillespie, A.R. eds., John Wiley & Sons, N.Y., N.Y., pp. 227-273.
- Nash, D., 1988, Detection of a buried horizon with a high thermal diffusivity using thermal remote sensing. *Photogrammetric Engineering and Remote Sensing* 54, 1437-1446.
- Price, J.C., 1977, Thermal inertia mapping: A new view of the earth. *Journal of Geophysical Research* 82, 2582-2590.
- Van Dam, R., Borchers, B., and Hendricks, J., 2005, Strength of landmine signatures under different soil conditions: implications for sensor fusion. *International Journal of Systems Science, Special Issue on Robots and Sensors for Landmine Detection*, 36(9), 573-588.

7 ACKNOWLEDGMENTS

This study was sponsored by the Department of the Army, Army Research Office (ARO contract number DAAD19-03-1-0159); the content of the information does not necessarily reflect the position or the policy of the federal government .